

Investigating Anion Selectivity of the GlyR Channel Using Imposed Voltage and Umbrella Sampling

Simon Pritchard^{a*}

^aStanford University, Department of Biology

Abstract: This research investigates the anion selectivity mechanisms of the glycine receptor (GlyR) channel using molecular dynamics simulations and umbrella sampling techniques. Building upon previous work, I examine the conductance properties and ion permeation characteristics of the transmembrane domain under various applied potentials, validating and building upon the prior findings of Dr. Seiferth [1] regarding GlyR channel properties. Potential of mean force (PMF) calculations reveal substantially higher free energy barriers for cations compared to chloride ions, providing a quantitative basis for the channel's anion selectivity. Additionally, I identified a significant interaction between chloride ions and the K292 residue at the extracellular end of the truncated transmembrane domain using hydration shell plots, highlighting limitations in using simplified channel models for MD simulations. These findings demonstrate both the utility and limitations of computational approaches in understanding ion channel selectivity mechanisms.

KEY WORDS Ion Channel, Glycine Receptors (GlyR), Ion Pore Domain, Molecular Dynamics, CHARMM-GUI, Positional Restraint, CHARMM36m, NBFIX, Potential of Mean Force (PMF), Umbrella Sampling, Free Energy, Hydration Shell

Received by Professor Phil Biggin on the 3rd January, 2025

1 Introduction

Ion channels are critical to the functioning of living cells, enabling the selective transport of ions such as sodium, potassium, and chloride across cell membranes. This selective permeability plays a key role in maintaining ionic balance, regulating cell volume, and controlling intracellular signaling pathways. In the nervous system, ion channels facilitate the rapid transmission of electrical signals between neurons. The structural and functional diversity of ion channels makes them a focal point for research into the molecular mechanics of ion channel function, their endogenous activity, and therapeutic applications for disease.

Glycine receptors (GlyRs) belong to the Pentameric Ligand-Gated Ion Channel (pLGIC) family and are crucial mediators of inhibitory neurotransmission in the central nervous system. By conducting chloride ions, GlyRs reduce neuronal excitability, playing a vital role in maintaining synaptic balance. These receptors are characterized by an ion pore domain embedded in a lipid membrane and an extracellular ligand-binding domain. Their selective permeability to chloride is key to their function, yet the underlying mechanisms of their selectivity, conductance, and gating remain active areas of investigation.

*Correspondence to: skpritch@stanford.edu

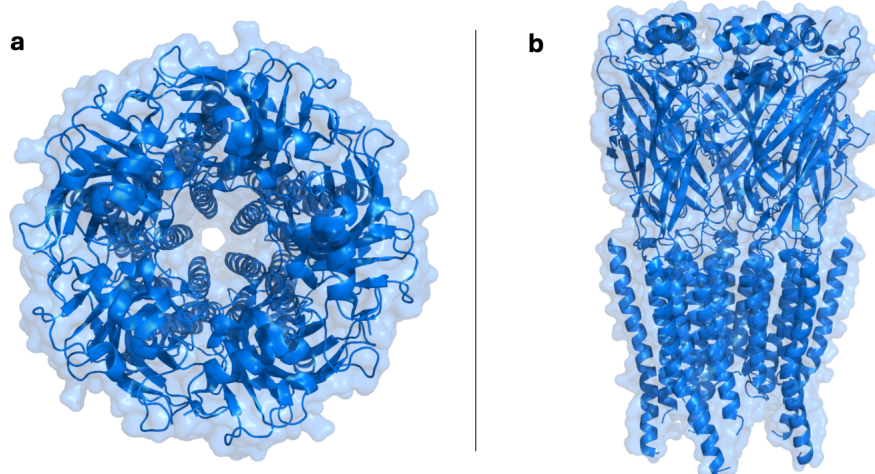


Figure 1: Cartoon representation of the $\alpha 1$ homomeric Glycine Receptor Channel (6pm2 model). (a) Top view. (b) Side view.

Molecular dynamics (MD) simulations have revolutionized the study of dynamic protein structure. In investigating the GlyR channel, MD simulations offer an atomistic view of ion behavior and pore dynamics impossible to achieve experimentally. Computational methods such as potential of mean force (PMF) calculations, hydration shell analyses, and conductance simulations allow for a closer evaluation of channel properties. These tools are more feasible when exploring truncated channel models, which isolate the transmembrane ion pore domain to reduce computational complexity.

Building on the work of Dr. David Seiferth [1], I examine the structural and functional properties of the GlyR ion pore domain. The research begins by replicating and validating key analyses of conductance, ion current, and permeation events in the GlyR pore. The robustness of the computational scripts used to analyze these properties is evaluated by testing their sensitivity to variations in assigned pore length. Furthermore, the relationship between applied potential and pore current is investigated to confirm its linearity under simulated conditions.

Anion selectivity is another focus, explored through PMF profiles for chloride, sodium, and potassium ions to examine differences in free energy landscapes across ion types. Hydration shell analyses corroborate such results and can be explanatory of the PMF topology. Finally, the study addresses artifacts introduced by the use of truncated channel models in simulations, evaluating their impact on the accuracy of PMF and hydration shell analyses.

2 Methods

2.1 Simulation Box Generation Using CHARMM-GUI

To generate the proper simulation conditions, CHARMM-GUI was used to take a membrane-embed-oriented protein (the 6pm2 GlyR channel for this work) and add a lipid bilayer, neutralizing ions, and water throughout the simulation box. To avoid the prohibitively high simulation cost of representing the entire channel, it was truncated prior to adding a membrane and solvating, such that only the transmembrane ion pore domain (AA 235–428) was represented. Omitting the extracellular ligand-binding domain was not expected to alter the behavior of ions during transit. The conductance of the channel depends on the rate-limiting step of permeation, which occurs in the transmembrane domain for the $\alpha 1$ homomeric GlyR channel according to Moroni et al. (2011) [2]. Moraga-Cid et al. (2015) [3] further demonstrated that replacing the extracellular domain of the $\alpha 1$ homomeric GlyR channel with that of GLIC results in identical permeation properties.

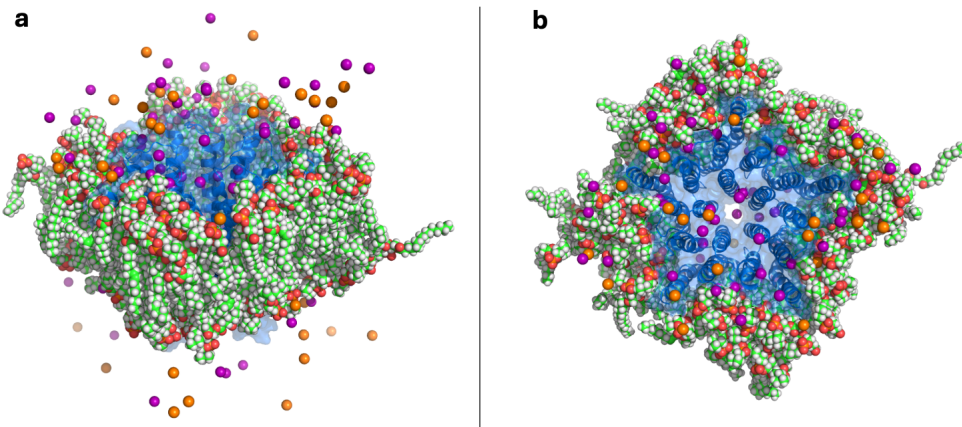


Figure 2: Illustration of the final simulation box (waters omitted) as generated by CHARMM-GUI. Transmembrane domain of GlyR channel in blue; ions in purple and orange. (a) Side view. (b) Top view.

1-palmitoyl-2-oleyl-sn-glycero-3-phosphocholine (POPC) lipids were used to create the membrane. chloride (Cl^{1-}) and either sodium (Na^{1+}) or potassium (K^{1+}) ions were added to a 150 mM concentration to achieve a neutralizing effect. Since the channel contains positive residues, this resulted in approximately 0.75 times more chloride ions than cations. The TIP3P water model was used, as is standard for simulation boxes generated with CHARMM-GUI. Prior work by Dr. Seiferth [1] demonstrated that the TIP4P model underestimates the channel’s conductance, while using TIP3P, along with NBFIX parameters (see Section 2.2) [5], provides a more accurate simulation.

2.2 Energy Minimization and Equilibration

Following simulation box generation, six 1ns simulations were conducted to minimize the possibility of a production run containing free energy instabilities. The following energy minimization and equilibration pipeline was taken from Dr. Seiferth’s prior simulation work. For exact parameters including simulation times, restraint magnitudes, and pressure/temperature settings see *Seiferth 2024* [1], section 3.3.1: Membrane System Equilibration Protocol.

Energy minimization of the protein–membrane system was conducted using the steepest descent integrator, with strong positional restraints applied to the backbone, side chains, and lipid phosphate groups. This procedure was set to converge when the maximum force dropped below a predetermined threshold or after 5000 steps, ensuring that the system reached a stable low-energy configuration. The Verlet cutoff scheme was employed to update the neighbour list, and electrostatic interactions were calculated using the Particle Mesh Ewald (PME) method, while hydrogen bonds were constrained with the LINCS algorithm. This minimized any unfavorable contacts before proceeding to equilibration.

A multi-step equilibration protocol was then implemented to gradually relax the system and ensure proper membrane configuration. The initial stages were performed in the NVT ensemble with strong positional restraints, which were progressively reduced in subsequent steps to allow controlled relaxation of the backbone, side chains, and lipid headgroups. The system was then transitioned to the NPT ensemble to account for pressure effects and further stabilize the membrane. In the final stage, minimal restraints were applied over an extended simulation to achieve a fully equilibrated state. Throughout these stages, temperature and pressure were maintained using Berendsen or velocity-rescaling thermostats and Berendsen or Parrinello–Rahman barostats, respectively. This systematic approach ensured that the membrane–protein system was well-equilibrated and suitable for subsequent production simulations.

2.3 Simulation Production Runs

To measure the conductance of the GlyR channel both the 6pm2 and Daemgen (as found in *Du et al., 2015* [4] and equilibrated under a protocol developed by Daemgen and Biggin) pores were simulated. As before, the simulation parameters were developed in *Seiferth, 2024* [1]; greater specifics can be found in section 3.4.1 of the thesis: CHARMM36m Simulations of Ion Channels in Membranes.

Ion channels embedded in membranes were simulated using the TIP3P water model and the CHARMM36m force field, incorporating pair-specific Lennard-Jones parameters (NBFIX) [5] to accurately represent chloride interactions with proteins, lipids, and alkali cations. Simulations were conducted using the GROMACS simulation engine, integrating Newton’s equations of motion with a leap-frog algorithm and a 2 fs time step.

The neighbor list was updated every 20 steps with the Verlet cutoff scheme, using a cutoff radius of 1.2 nm. Van der Waals interactions employed a force-switching scheme starting at 1.0 nm and turning off at 1.2 nm, while electrostatic interactions were calculated with the Particle Mesh Ewald (PME) method. Temperature was maintained at 310 K with the velocity-rescaling algorithm, employing separate coupling groups for the solute, membrane, and solvent. Pressure was managed semi-isotropically using the Parrinello-Rahman barostat, with a reference pressure of 1.0 bar and an isothermal compressibility suitable for water.

Hydrogen bonds were constrained using the LINCS algorithm, enabling a larger time step by maintaining bond geometry. Reference coordinate scaling was applied to the center of mass when restraints were required on the protein to preserve specific conformations. To ensure system stability, center of mass motion was removed every 100 steps for the solute, membrane, and solvent using a linear center of mass removal algorithm. This combination of parameters ensured accurate and stable simulations of the ion channel within its membrane environment.

2.4 Calculating Channel Properties

Pores were simulated for 250 ns to ensure a more accurate estimate of the channel properties. When permeation events are modeled as a Poisson distribution, the variance of the estimate decreases proportionally to the length of the simulation, thereby improving statistical reliability. A 500 mV potential was applied along the positive z-axis to drive chloride permeation. It is worth noting that—though common practice in MD simulations—a steady 500 mV potential is inconsistent with the dynamic potential exhibited across cell membranes and significantly exceeds typical endogenous potentials.

The MDAnalysis package in Python was employed to analyze the production run output files. The calculated conductance values for both the 6pm2 and Daemgen pores were well within experimental ranges, measuring 99.11 picosiemens (pS) and 101.14 pS, respectively.

The stability of conductance estimation scripts was then examined with respect to defined pore lengths. The conductance analysis script was iteratively applied to increasing pore lengths (centered at the COM of the protein), and conductance and ion transit events were measured for each configuration. Because the boundaries of the pore along the z-axis can be defined in a relatively arbitrary manner, I hypothesized that the choice of boundaries would significantly impact how precisely ion transits would be counted, impacting the conductance estimates.

To investigate the effect of voltage on ion current through the GlyR channel, simulations were performed under various symmetric potentials (-500 mV, -250 mV, 250 mV, 500 mV). The resulting currents were calculated to assess the potential for a nonlinear relationship between voltage and current. The ± 250 mV simulations were extended to 500 ns to ensure a stable estimate of permeation events.

2.5 Potential of Mean Force Calculations (PMFs)

To evaluate the chloride selectivity of the GlyR channel, potential of mean force (PMF) profiles were generated for chloride (Cl^{1-}), sodium (Na^{1+}), and potassium (K^{1+}) ions. The expectation was that the free energy landscape for the cations would exhibit insurmountable free energy barriers, explaining the channel's selectivity against them. Umbrella sampling was employed to accurately quantify the forces acting on ions at each respective point along the channel. Sampling windows were configured with sufficient overlap to allow for the reconstruction of a continuous free-energy profile. All PMF calculations were performed using the 6pm2 pore.

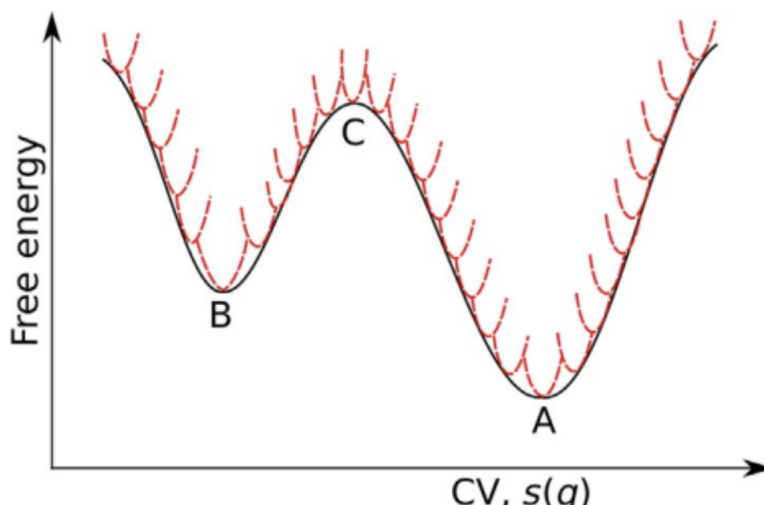


Figure 3: Representation of umbrella sampling taken from Ghosh et al., 2024 [6]. Each overlapping distribution represents a simulation window with imposed restraints to create a stable-equilibrium free-energy environment.

The standard approach for generating a PMF profile involves "pulling" an ion through the channel while applying restraints to ensure thorough sampling along the pull axis. However, this technique can inadvertently introduce biases by preserving information from prior time steps, influencing subsequent sampling windows. To mitigate this issue, an alternative approach was implemented: a random ion in the simulation box was selected, and at a series of coordinates along the z-axis (spaced at 1 Å intervals down the channel center), a water molecule and the chosen ion were swapped.

This method represents a deviation from the approach used in Seiferth, 2024 [1], in which the water molecule was simply deleted rather than swapped with the ion. By exchanging the water molecule and ion positions, the need to regenerate an index file for each simulation window's .gro file was eliminated. Additionally, the radius in the xy-plane used for generating sampling windows differed from that in Dr. Seiferth's prior work [1]. While his method utilized a 7 Å radius centered on the pore's center of mass (COM), this study employed a 5 Å radius, resulting in a more precisely centered series of ions across sampling windows.

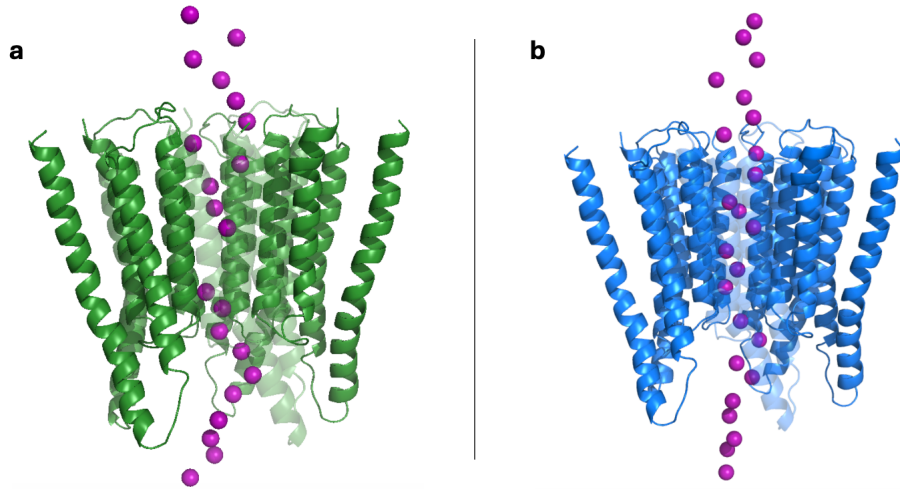


Figure 4: Comparison for starting configuration xy radius. (a) 7 Å radius generates a less centered stream of ions through the channel. (b) 5 Å radius creates a more precise set of sampling window starting configurations.

To prepare each sampling window for production runs, a 1 ns equilibration simulation was conducted under an NPT ensemble, as outlined in Section 2.2, to ensure stability following the ion-water swap. The umbrella sampling itself consisted of a 21 ns production run with parameters similar to those detailed in Section 2.3, except that no external potential was applied to the simulation box. The GROMACS pull function was used to impose positional restraints on the selected ion, but no pull force was applied along the z-axis, as each sampling window was treated independently.

2.5.1 PMF Analysis

The Weighted Histogram Analysis Method (WHAM) was used to generate PMF profiles from the sampling windows based on the production run trajectory files. The currently accepted approach for creating PMF profiles involves cyclizing the free energy reconstruction, ensuring that the PMF values at the start and end of the trajectory are equivalent. This equivalence reflects the expectation that the force on an ion (or other simulated entity) should be the same in bulk solvent at the boundaries of the simulation. However, due to noise and variance inherent to molecular dynamics simulations, this equivalence is not guaranteed.

To enforce this boundary condition, the -cycl flag in WHAM can be applied, which forces the start and end PMF values to match. While this adjustment may reduce inconsistencies at the boundaries, it can also significantly alter the overall PMF profile, potentially affecting the accuracy of the results.

To evaluate the impact of cyclizing the PMF profiles on their accuracy, WHAM was executed on the trajectory files for all three ions (Cl^{1-} , Na^{1+} , and K^{1+}) with and without the -cycl flag. The resulting profiles were compared to assess the effect of this clamping procedure on the free energy reconstructions.

2.5.2 Hydration Shells

Hydration shell profiles for chloride (Cl^{1-}), sodium (Na^{1+}), and potassium (K^{1+}) ions were analyzed using the umbrella sampling runs. The hydration profiles were calculated by determining, for each time step and each

sampling window, the number of water hydrogens, water oxygens, and protein hydrogens within a specified radius of the ion.

For chloride ions, the radii used were 2.75 Å, 3.75 Å, and 3.0 Å for water hydrogens, water oxygens, and protein hydrogens, respectively. For sodium and potassium ions, the selected radii were approximately 15% smaller than those for chloride, reflecting their smaller ionic radii and corresponding hydration shells.

3 Results

3.1 Effect of Analysis Setup on Conductance Calculations

In replicating Dr. Seiferth's work on GlyR channel properties, the robustness of the analysis scripts was investigated. As described previously, the choice of transmembrane domain length was hypothesized to have a significant impact on the measured properties due to its influence on how ion transits are calculated. To assess this, conductance and the number of ion transits were plotted as a function of steadily increasing pore lengths, centered on the protein COM.

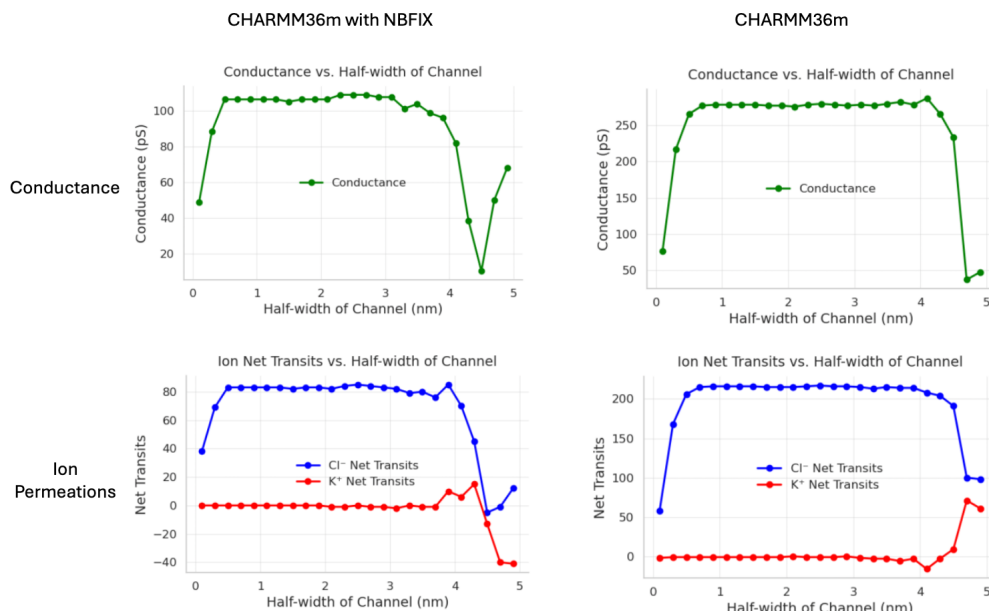


Figure 5: Robustness analysis for defined 6pm2 pore length in conductance estimates. Conductance and anion/cation permeation events for increasing transmembrane domain length as set in analysis scripts.

As shown in Figure 5, the analysis method demonstrates remarkable robustness across pore lengths ranging from approximately 1 nm to 6 nm (0.5 nM to 3 nM half-width). Notably, the transmembrane domain of the GlyR channel is approximately 3.5 nm in length, providing the analysis script with substantial error tolerance. Extending the pore boundaries beyond the membrane bilayer (up to a half-width of 3 nm) yields conductance estimates nearly identical to those derived from the actual protein boundaries. Instabilities arise only when the half-width is less than 0.5 nm—where ion transits occur faster than they can be measured—or greater than 3 nm, where an excessive portion of the 10.5 nm simulation box is erroneously classified as "transiting," leading to underestimation.

3.2 GlyR Pore Shows a Linear Relationship Between Voltage and Current

The interaction between the applied voltage magnitude and the resulting pore current was also examined. Four distinct voltages were tested, and the current was estimated for each simulation. Using ordinary least squares (OLS) regression to fit a trendline revealed an almost perfectly linear relationship between voltage and current. The trendline was constrained to pass through the origin, as the channel current is expected to be zero under conditions of no applied potential.

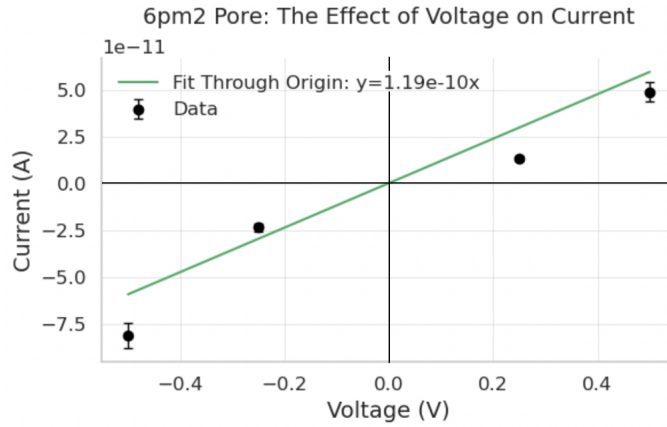


Figure 6: 6pm2 pore current as a function of increasing applied voltage.

3.3 Cation PMFs Show Higher Free Energy Barrier to Permeation

To investigate the anion selectivity of the GlyR channel, PMFs were generated for chloride (Cl^{1-}), potassium (K^{1+}), and sodium (Na^{1+}) ions transiting the 6pm2 pore, as described in Section 2.5. As shown in Figure 7, the chloride PMF exhibited two major free-energy barriers, each approximately 2 kcal/mol in magnitude. These barriers align with the P-2' and L9' residues, which have been identified as key contributors to GlyR channel gating and selectivity, as described by Dr. Seiferth in his thesis [1].

As anticipated, the PMFs for the cations, potassium and sodium, displayed significantly higher free-energy barriers to permeation, with the largest barrier measuring 7 kcal/mol and 6 kcal/mol, respectively. The primary barrier for cation permeation, located at -15 \AA , is attributed to interactions between the cations and the positively charged amine group on the P-2' residue.

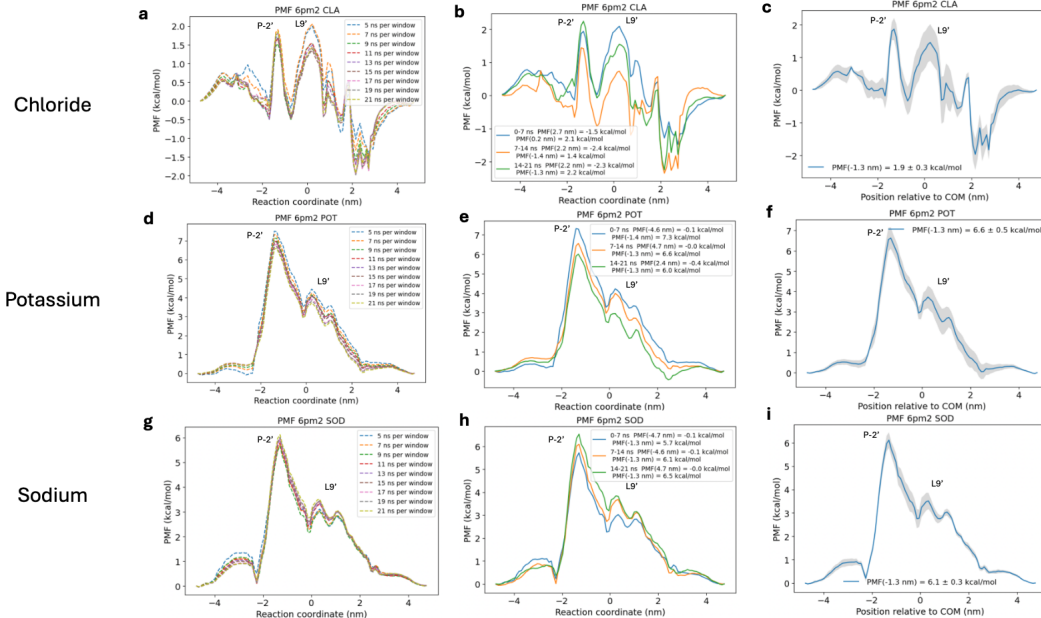


Figure 7: PMF profiles for the 6pm2 pore illustrating convergence across time-steps for (a-c) chloride (Cl^{1-}), (d-f) potassium (K^{1+}), and (g-i) sodium (Na^{1+}).

3.4 Effect of Chloride Interaction with Extracellular Pore Residues on PMFs

Hydration shell plots were generated for chloride (Cl^{1-}), potassium (K^{1+}), and sodium (Na^{1+}) ions transiting the 6pm2 pore, as illustrated in Figure 8. As anticipated, the chloride ion exhibits some degree of "dewetting" around the P-2' gate, consistent with prior findings in *Seiferth, 2024* [1]. This dewetting is indicated by a reduction in the hydration shell and an increase in interactions with protein atoms. Similar hydration shell stripping is observed for the cations, although their interactions with protein atoms are generally repulsive.

More notably, chloride ions exhibit more pronounced hydration shell stripping and a significant increase in interactions with protein atoms at the extracellular end of the transmembrane domain. This region, located

approximately 20–30 Å above the COM of the pore, corresponds to a previously undetermined free-energy valley in the chloride PMF, with a depth of -2 kcal/mol.

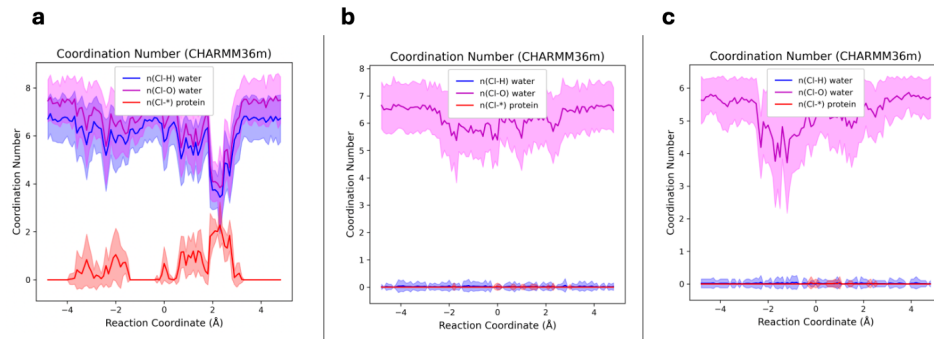


Figure 8: Hydration plots of the interaction numbers for (a) chloride (Cl^{1-}), (b) potassium (K^{1+}), and (c) sodium (Na^{1+}) for each sampling window along the 6pm2 pore.

Visualization of the simulation results reveals that the chloride ion, for the simulation windows around 23 Å, interacts with the positively charged residue K292. Notably, a pocket is observed at the extracellular end of the transmembrane domain, where the chloride ion can reside. This pocket is clearly depicted in Figure 9.

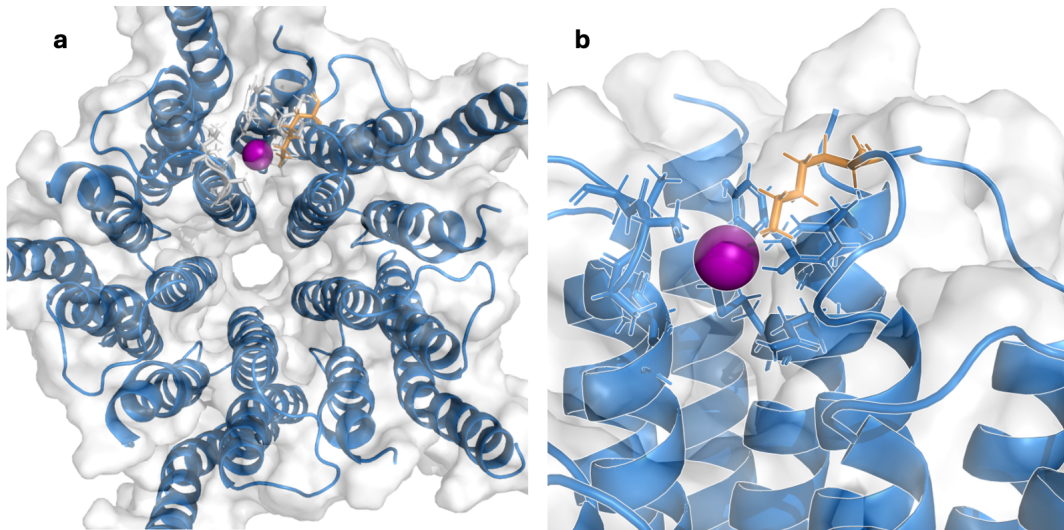


Figure 9: Interaction between positive K292 (in orange) and chloride ion (in purple) at 23 Å. (a) Top view. (b) Side view.

The interaction between the transiting ion and charged residues within the pore is observed exclusively in the PMF and hydration shell analysis for chloride (Cl^{1-}). As shown in Figure 10, chloride is the only ion to exhibit a significant interaction with a specific region of the channel, highlighted by the red arrow. In all other sampling windows, the ions are either aligned along the central channel axis or randomly distributed in bulk solvent, (no xy-plane restraints were applied during the simulations).

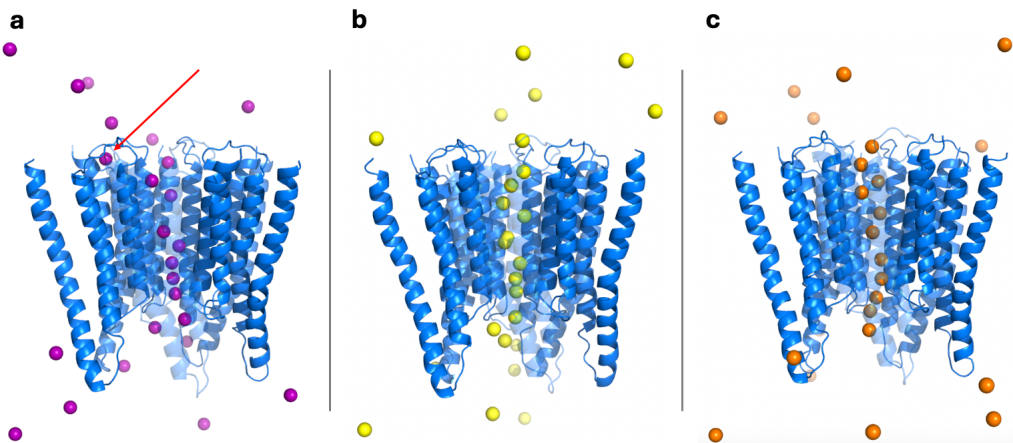


Figure 10: Final positions across simulation windows along the 6pm2 pore for (a) chloride (Cl^{1-}) (b), sodium (Na^{1+}), and (c) potassium (K^{1+}).

Although not particularly relevant for calculating channel properties—since only ions restrained along the z-axis form the specific K292 interaction while transiting or returning to bulk solvent—this interaction significantly affects the accuracy of the PMF, particularly when cyclizing the profile. As discussed in Section 2.5.1, cyclizing the PMF profile is essential to achieve symmetry in the free-energy landscape reconstruction in bulk solvent on either side of the membrane.

As illustrated in Figure 11, the chloride PMF demonstrates the most pronounced differences between profiles generated with and without enforced cyclizing, suggesting greater potential inaccuracies in the cyclized PMF. In contrast, the potassium and sodium PMFs exhibit minimal differences, indicating less susceptibility to inaccuracies due to interactions with pore residues. Notably, if the full GlyR channel were simulated, these PMF inaccuracies would likely disappear. While a free-energy valley might still exist, it would be positioned approximately halfway along the channel and would not disrupt the enforced symmetry of the PMF in bulk solvent. However, due to the truncation of the channel to make the simulation computationally feasible, this interaction now has an outsized impact on the accuracy of the PMF profile. Additionally, it introduces artifacts into the hydration profile analyses, further complicating the interpretation of results.

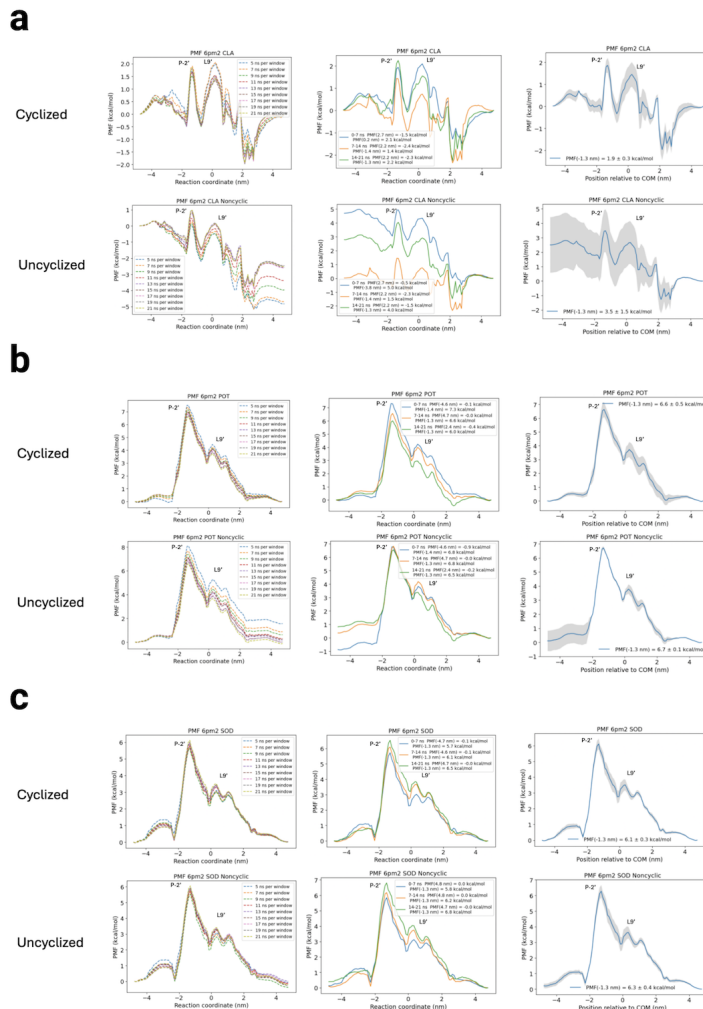


Figure 11: Cyclized and uncyclized PMF profiles for (a) chloride (Cl¹⁻), (b) potassium (K¹⁺), and (c) sodium (Na¹⁺).

4 Discussion

The molecular dynamics simulations conducted here successfully reproduced and validated Dr. Seiferth's findings regarding GlyR channel properties [1]. The robustness analysis demonstrated remarkable stability in conductance calculations across pore lengths ranging from 1 nm to 6 nm, far exceeding the actual transmembrane domain length of around 3.5 nm. This stability, combined with the observed linear relationship between applied voltage and channel current, confirms the reliability of the Biggin lab's computational approach and suggests that the simulation parameters effectively capture the dynamics of ion permeation through the channel.

The PMF calculations provide a quantitative explanation for the channel's anion selectivity, revealing substantially higher free energy barriers for sodium and potassium ions compared to chloride. While chloride ions encounter modest barriers of approximately 2 kcal/mol near the P-2' and L9' residues, cations face significantly higher barriers of 6-7 kcal/mol. These energetic differences, supported by hydration shell analyses, demonstrate the molecular basis for the channel's preferential conduction of anions over cations.

Analysis of the truncated transmembrane domain revealed significant limitations in using simplified channel models for MD simulations. As shown in Figure 12, the truncation of the channel affects the positioning of the K292 residue, allowing it to form an artificial interaction with chloride ions during umbrella sampling. In the complete channel structure, K292 forms a polar contact with Y239, adopting a conformation that precludes this interaction. This artifact significantly impacts both PMF profiles and hydration shell analyses, especially at the extracellular end of the truncated domain, highlighting the importance of identical structural context in computational studies of ion channels.

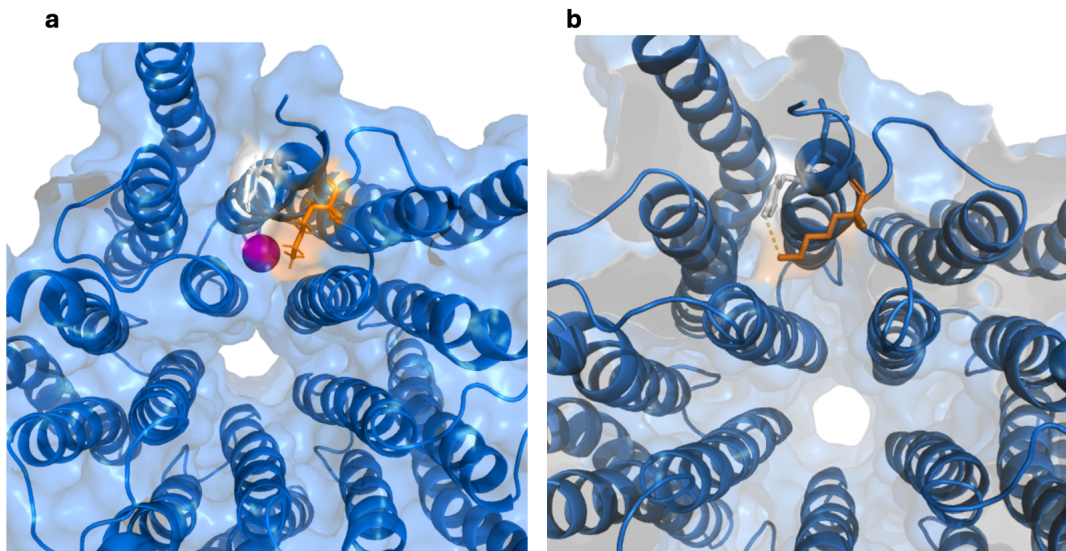


Figure 12: Position of K292 in the (a) truncated (with chloride at 23 Å) and (b) untruncated 6pm2 channel. K292 in orange; Y239 in white.

5 Conclusion

This research successfully validated previous conductance measurements for the GlyR channel while demonstrating the robustness of computational methods across various analysis parameters. It provided quantitative evidence for anion selectivity through PMF calculations, revealing substantially higher free energy barriers for cations compared to chloride ions. Hydration shell analyses further supported these findings, showing characteristic patterns of ion-protein interactions that explain the selective permeation of anions. The study also identified important limitations in using truncated channel models, particularly regarding artificial interactions between ions and terminal residues. These findings both validate the prior work done on the properties of ion channels using MD simulations and highlight important concerns regarding simplifying assumptions made for computational feasibility.

Acknowledgment

Thank you to Professor Phil Biggin for allowing me to join the Biggin Lab for Michaelmas, 2024—it would have been impossible to do any of this work otherwise. Thank you, as well, to Dr. David Seiferth for his guidance on running MD simulations, and for providing many of the base files used here.

References

- [1] Seiferth, D. (2024). Functional annotation using molecular dynamics: A journey into ion channel function. Oxford University.
- [2] Moroni, M., et al., (2011). Chloride ions in the pore of glycine and GABA channels shape the time course and voltage dependence of agonist currents. *Journal of Neuroscience*, 31(40), 14095–14106. <https://doi.org/10.1523/JNEUROSCI.3158-11.2011>
- [3] Moraga-Cid, G., et al., (2015). Allosteric and hyperekplexic mutant phenotypes investigated on an $\alpha 1$ glycine receptor transmembrane structure. *Proceedings of the National Academy of Sciences*, 112(9), 2865–2870. <https://doi.org/10.1073/pnas.1417209112>
- [4] Du, J., et al., (2015). Glycine receptor mechanism elucidated by electron cryo-microscopy. *Nature*, 526(7572), 224–229. <https://doi.org/10.1038/nature14853>
- [5] Orabi, E. A., et al., (2021). Corrections in the CHARMM36 parametrization of chloride interactions with proteins, lipids, and alkali cations, and extension to other halide anions. *Journal of Chemical Theory and Computation*, 17(10), 6240–6261. <https://doi.org/10.1021/acs.jctc.1c00780>
- [6] Ghosh, D., Biswas, A., & Radhakrishna, M. (2024). Advanced computational approaches to understand protein aggregation. *Biophysics Review*, 5(021302). <https://doi.org/10.1063/5.0180691>

- [7] KALP-15 in DPPC. Retrieved December 13, 2024, from www.mdtutorials.com/gmx/membrane_protein/index.html
- [8] Lemkul, J. A., & Bevan, D. R. (2010). Assessing the stability of Alzheimer's amyloid protofibrils using molecular dynamics. *The Journal of Physical Chemistry B*, 114(4), 1652–1660. <https://doi.org/10.1021/jp9110794>
- [9] Lysozyme in water. Retrieved December 13, 2024, from www.mdtutorials.com/gmx/lysozyme/index.html
- [10] OpenAI. (2024). GPT-4 technical report. Retrieved from <https://openai.com/research/gpt-4>
- [11] Umbrella Sampling. Retrieved December 13, 2024, from www.mdtutorials.com/gmx/umbrella/index.html